

Design Analysis and Fabrication of High Gain Wideband Antipodal Vivaldi Antenna for Satellite Communication Applications

Nitin Muchhal^{*#}, Renato Zea Vintimilla^{*}, Mostafa Elkhoully^{*}, Yaarob Fares^{*}, Shweta Srivastava[#]
^{*}Fraunhofer Institute for Integrated Circuits IIS, Am Wolfsmantel 33, 91058 Erlangen, Germany
 {firstname.lastname@iis.fraunhofer.de}^{*}

[#]Jaypee Institute of Information Technology Noida, India
 {shweta.srivastava@jiit.ac.in}

^{*#}corresponding author e-mail: nmuchhal@gmail.com

Abstract — A wideband and high gain corrugated epsilon negative index metamaterial (ENG) Antipodal Vivaldi Antenna (AVA) with gain >12 dBi and working in frequency range from 10 GHz - 25 GHz (for SATCOM applications) is proposed in this paper. The overall performance of the proposed Antipodal Vivaldi Antenna (AVA) is enriched by using a triangular shaped corrugation slots and pi (Π) shaped epsilon negative metamaterial cells. The 'Γ' shaped metamaterial unit cells are positioned on the upper surface amid both radiators of AVA to emanate the intense electric field in the end-fire direction. The proposed antenna size is 22.6 mm × 15.8 mm x 1.6 mm and it is designed on the FR4 substrate. The proposed antenna is then fabricated using photolithography process and tested for its performances. There is good agreement between simulated and measured results. The measured gain varies from 6.2 – 10.7 dBi.

Keywords- Metamaterial; Corrugation; Antipodal Vivaldi Antenna (AVA); Gain; SATCOM.

I. INTRODUCTION

Wideband antenna with high gain is the primary requisite for any communication system. Such a high gain wideband antenna is recently proposed in [1]. Furthermore, high data rates and increased quality of service (QoS) for end users are in ever-increasing demand due to the recent improvement and spectacular achievement in the field of wireless communication technology [2], [3]. Wireless communication system designers face a challenging task when designing compact and wideband antenna for high-speed, high-capacity, and secure wireless communications. In contemporary times numerous designs of wideband antennas fulfilling varied objectives have been proposed by various researchers for modern wireless networks [4-6].

To accomplish pervasive connectivity on the globe, SATellite COMmunication (SATCOM) is a crucial constituent of next-generation wireless communications. Also, SATCOM is one of the leading technologies used today for high speed internet communication [7]. Ku-band that is a part of the electromagnetic spectrum, which operates in frequency range from 12 GHz to 18 GHz, is one of prominent and widely used frequency band for satellite communication in the world. It is considered trustworthy for

the high-powered satellite services used in digital TV, teleconferences, vehicular communication, entertainment, and international programming [8],[9]. Also, they find huge application in Very Small Aperture Terminal (VSAT) [10] systems on ships, commercial aircraft, etc.

In recent times, a significant amount of research work has been proposed to design various vital components [11-13] for SATCOM applications. The Vivaldi antenna was proposed and designed by Gibson for high-frequency applications [14]. Later, Gazit improved it by giving it an antipodal shape to enhance the bandwidth and gain [15]. By incorporating numerous enhancement methods, e.g., adding parasitic patch, dielectric lens, array and metamaterial, the parameters of the Antipodal Vivaldi Antenna (e.g., directivity, bandwidth, reduction inside lobe level, etc.) can be improved. Agahi et al. [16] proposed a novel scheme for enhancing the performance of AVA by integrating two small parasitic patches inserted adjacent to the conventional flare structure to make the current distribution stronger. The addition of the parasitic patches augment the bandwidth, nonetheless, the gain performance is not much improved. Moosazadeh et al. [17] proposed a high gain AVA. To enhance gain at lower frequencies, first slit edge technique is applied to conventional antipodal Vivaldi antenna (CAVA). Furthermore, a trapezoid dielectric lens is appended to improve the gain and directivity at higher frequencies. The dielectric lens used upsurges the end-fire radiations, but at the cost of a large size. Dixit et al. [18] proposed 1 x 4 AVA array (AVA-A) designed with apertures amid two antenna elements. Further performance of AVA-A is boosted by incorporating corrugations in it. The proposed AVA Array design improves the gain but suffers from augmented mutual coupling due to proximity of antenna elements. A wide-band and compact Antipodal Vivaldi Antenna (AVA) was proposed by Zhang et al. [19] for use in ultra wideband applications. To make the AVA smaller, an arc curve is used in place of the radiator's exponential tapering edge. The AVA also has a "director" and a "convex lens" to increase its gain at high frequencies. The proposed antenna has a small size and operates in the 3.01 to 10.6 GHz frequency range but it has a drawback of complex design and fabrication. Dixit et al. [20] proposed a 1 × 4 AVA array for numerous 5G services. The proposed

antenna has a high gain and works in the frequency bands 24–29 GHz and 30–40 GHz, respectively; nonetheless, it has large size due to multiple array elements. A novel technique was proposed by Nassar et al. [21] to improve the bandwidth and directivity of broad band (2 GHz - 32 GHz) antipodal Vivaldi antenna configuration. The technique is based on adding a parasitic elliptical patch to the aperture to increase field coupling between the arms and create additional radiation in the direction of the end fire, still it has low gain. Emre et al. [22] proposed an UWB Vivaldi antenna array with high gain for Synthetic Aperture Radar applications. First, the single element of antenna is designed for ultra-wide band operation in the X and Ku-band frequency range. Afterward, the proposed antenna is then shielded from surface currents by edge grooves made on the sides of the exponential etched patch surface. Additionally, the parasitized element is supplemented to improve antenna gain still due to ineffective coupling, radiation properties are not good. Cheng et al. [23] proposed a miniaturized Vivaldi Antenna for Ground Penetrating Radar system. In the proposed design, an Artificial Materials Lens (AML) and a Side Lobe Suppressor (SSR) are implanted to enhance the gain and radiation properties of the GPR antenna. The higher frequency of EM waves is affected by AML, whereas the lower frequency of EM wave is affected by SSR but design is quite complex.

Amongst several techniques, the enhancement technique using metamaterial is quite effective without increasing the size of an antenna [24],[25]. After an intensive literature review, it is established that little work is done on AVA with metamaterial for SATCOM applications. This paper presents a compact and enhanced gain AVA with π shaped metamaterial for SATCOM applications.

The rest of the paper is structured as follows: Section I covers introduction and literature review of Vivaldi antenna. Section II briefly discusses about Vivaldi antenna. Section III elaborates on the design of the proposed conventional AVA. Section IV deals with the design of the corrugated AVA. Section V covers the design and analysis of corrugated AVA with the novel metamaterial unit cells. The simulated results of the proposed AVA are discussed in Section VI. Section VII deals with the fabricated design and measured results. The outcomes of the proposed AVA are concluded in Section VIII followed by references.

II. VIVALDI ANTENNA

Vivaldi antenna is a traditional UWB antenna possessing wide bandwidth, high efficiency and small size. Vivaldi antenna's early design was unveiled by Gibson in 1979 [4]. Figure 1 depicts the generalized structure of microstrip fed tapered slot Vivaldi antenna. It is essentially a flared slotline that is fabricated on a single metallization layer reinforced

by a dielectric substrate. The tapered profile conventionally has exponential curve that generates a smooth transition from the slotline to the open space.

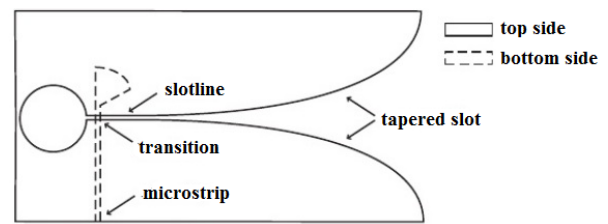


Figure. 1 Tapered slot Vivaldi antenna [26]

The tapered-slot antennas employ a traveling wave propagating along the antenna structure since the phase velocity is less than the velocity of light in free space. Therefore, they create radiation in the endfire direction at the broader end of the slot in preference to other directions [27].

III. DESIGN OF CONVENTIONAL AVA (CAVA)

Antipodal Vivaldi Antenna (AVA) was first proposed by Gazit in 1988. It unveils superior features such as wideband, high gain, stable radiation pattern and easy fabrication and hence it can efficiently gratify the various requirements of SATCOM. It consists of tapered or exponential metallic patches on top and bottom plane with a microstrip feed line matching with the connector, as shown in Figure 2.

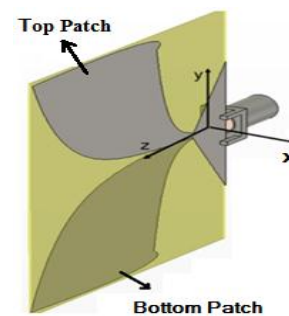


Figure 2. Antipodal Vivaldi Antenna [28]

Figure 3 depicts the geometry of the Conventional Antipodal Vivaldi Antenna (CAVA) simulated in HFSS ver. 13. This antenna consists of two parts: elliptical curved radiation flares and feed line. The top and bottom patches act as radiator and ground, respectively. The antenna is designed on standard and economical substrate FR4 with a dielectric constant of 4.4, $\tan \delta$ as 0.02 and thickness 1.6 mm and simulated using HFSS ver. 13. As the Antipodal antennas operate as a resonant antenna at the lower end of frequency band, the antenna length L_1 and width W_1 are determined based on the lowest frequency f_L , relative

dielectric constant ϵ_r . The antenna dimensions are calculated by using the following equations [28]:

$$L_1 = \frac{c}{f_L} \sqrt{\frac{2}{\epsilon_r + 1}} \quad (1)$$

$$W_1 = \frac{c}{2f_L \sqrt{\epsilon_r}} \quad (2)$$

The curve equations are given as

$$Y = \pm(R_1 e^{rx} + R_2) \quad (3)$$

where R1 and R2 are given by:

$$R_1 = \frac{y_2 - y_1}{e^{rx_2} - e^{rx_1}} \quad (4)$$

$$R_2 = \frac{e^{rx_2} y_1 - e^{rx_1} y_2}{e^{rx_2} - e^{rx_1}} \quad (5)$$

Here, R1 and R2 are constants, 'r' symbolizes the increase rate of an exponential curve and, x1, y1, are the initial points and x2, y2 are the termination points of the exponential curve.

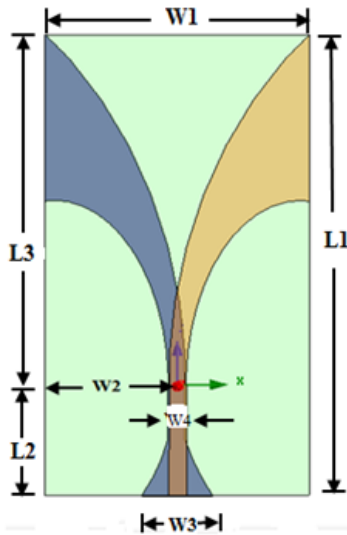


Figure 3. Structure of CAVA

The dimensions of the CAVA are calculated to have an optimized response over the desired bandwidth and they are found to be as follows: L1= 22.60 mm, L2 = 5.50 mm, L3= 17.1 mm, W1= 15.8 mm, W2= 7.2 mm, W3= 4.2 mm. The width of the microstrip feedline (W4) is calculated to match the characteristic impedance of 50 ohm which comes out to be W4= 1.25 mm. The radiating structure of the antenna is formed from the intersection of quarters of two ellipses, as explained in [29].

Figure 4 depicts the S11 response for the CAVA. From the curve, it can be seen that the designed CAVA resonates below -10 dB in the range of 10.8 GHz to more than 25 GHz.

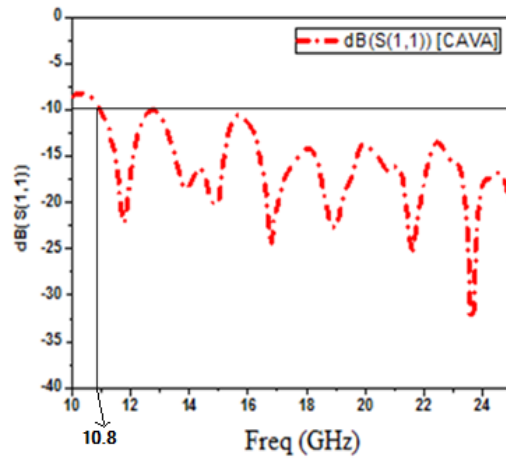


Figure 4. Frequency response of CAVA

Figure 5 shows the gain for the conventional AVA (CAVA). It is evident from Figure 4 that CAVA achieves low values of gain mainly at lower frequencies with maximum gain of 5.8 dBi only towards higher frequency.

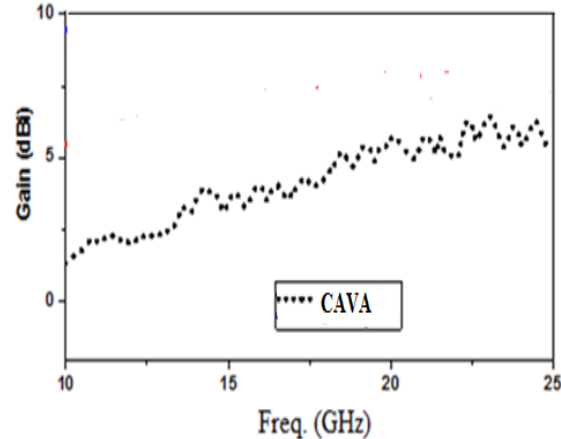


Figure 5. Gain plot of CAVA

Since the proposed CAVA dispenses low gain at lower frequencies, corrugation can be used to overcome this problem [30]. This will be explained in detail in Section IV.

IV. DESIGN OF CORRUGATED AVA

The low frequency performance of an AVA flare is enriched by the corrugation on its outer edges. Figure 6 depicts the design of the equilateral triangular corrugated AVA with slot side length, S = 0.85 mm.

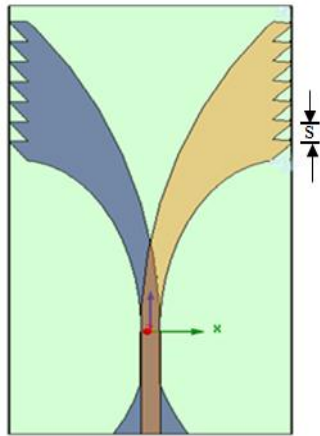


Figure 6. Structure of Corrugated AVA

The simulated S11 response of corrugated AVA is depicted in Figure 11. It can be seen that by adding corrugation, the lower cutoff frequency shifts to 10.3 GHz. The reason behind this shift in frequency is that the slot corrugation facilitates the electrical length of the inner taper profile to be elongated thereby extending the lower end cut-off frequency [31]. Further, the corrugation acts as a high impedance region due to which the maximum surface current remains towards the inner edge of the tapered slot reducing side and backlobe radiation, increasing the gain in boresight direction [32].

To further enhance the gain and improve the radiation characteristics, an array of metamaterial is commonly used on AVA aperture [33]. This will be explained in detail in Section V.

V. DESIGN AND ANALYSIS OF CORRUGATED AVA WITH METAMATERIAL (MTM)

To enhance the gain and characteristics of the proposed Vivaldi antenna, an array of epsilon negative metamaterial (ENG) unit cells is supplemented at its aperture. The proposed 'pi shape (π)' metamaterial is shown in Figure 7. The proposed MTM is placed inside a waveguide with Perfect Magnetic Conductors (PMC) on its top and bottom, Perfect Electric Conductors (PEC) on its side walls and two waveguide ports for excitation [34], as shown in Figure 8. Standard retrieving procedure is followed by using transmission and reflection coefficient of the unit cell, as described in [35], and it is found that the proposed metamaterial unit cell exhibits epsilon negative property, as shown in Figure 9. The optimized dimensions (in mm) of unit cell are as follows: $A = 1.6$, $B = 0.25$, $C = 1.35$, $D = 0.70$.

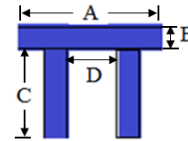
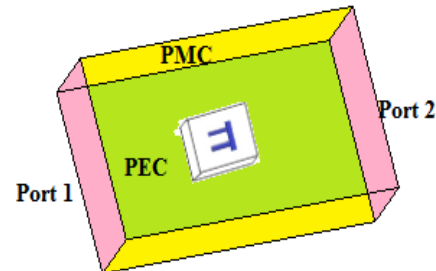
Figure 7. π shape Metamaterial Unit Cell

Figure 8. Simulation model of the proposed unit cell

Figure 8 illustrates the ENG behavior of the unit cell with negative relative permittivity property in range of 14 GHz - 18 GHz.

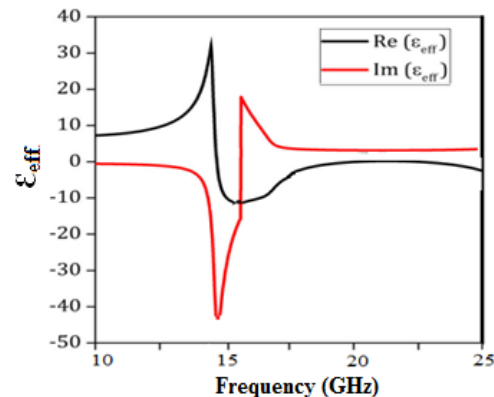


Figure 9. Permittivity graph of ENG unit cell

The MTM array was supplemented to the upper side of the antenna radiating aperture to augment the performance of the corrugated AVA. Using [36] and analyzing by various placements and numbers of the proposed metamaterial cells for the desired frequency range, it was found that the proposed design with six MTM cells at 3-2-1 arrangement (from the top), as shown in Figure 10, attains the preferred bandwidth with better gain radiating maximum energy in the end-fire direction, as will be discussed in Section VI.

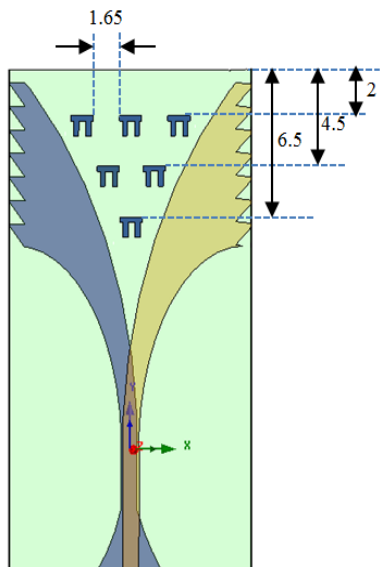


Figure 10. Corrugated AVA with Metamaterial (MTM) unit cells

VI. SIMULATED RESULTS AND DISCUSSION

Figure 11 illustrates the simulated results of reflection coefficient (S_{11}) with frequency for the corrugated AVA and corrugated MTM AVA. As can be noticed from the figure, the reflection coefficient of the corrugated AVA is below -10 dB for the frequency range of 10.3 GHz to 25 GHz. Applying the corrugation technique resulted in extension of the lower end frequency limit due to elongation of inner taper length. The negative index metamaterial further ameliorated the lower cut-off frequency making $S_{11} < -10$ dB for the entire range from 10 GHz - 25 GHz.

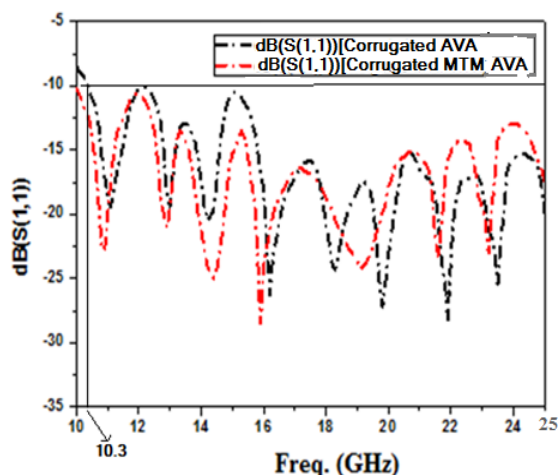


Figure 11. Comparison of Frequency response of Corrugated AVA and Corrugated MTM AVA

Figure 12 depicts the comparison of the gain plot of Corrugated AVA and Corrugated MTM AVA. The Corrugated AVA provides gain in the range of 6.5 dBi - 8.6 dBi, whereas the AVA-M provides the gain in the range of 7.3 dBi - 12.2 dBi with maximum gain achieved at 14.5 GHz. As evident from the gain plot, by integrating corrugation on both side edges of conducting arms, the gain of the proposed antenna increased significantly, especially at the lower end of the operating frequency band. Further, by integrating the metamaterial unit cells structure, the gain enrichment is more pronounced in the mid frequency band. Hence, the peak gain is enhanced by approximately 3.8 dBi in the desired range after inclusion of metamaterial unit cells, which is a significant gain enhancement without changing the antenna size. Also, as observed from Figure 11, the gain is maximum towards the center frequency and drops towards lower and higher frequencies. Since, gain is dependent on the matching, and it is matched at mid-frequency ranges, therefore, it may be getting worse at higher and lower frequency ranges, causing a reduction in gain.

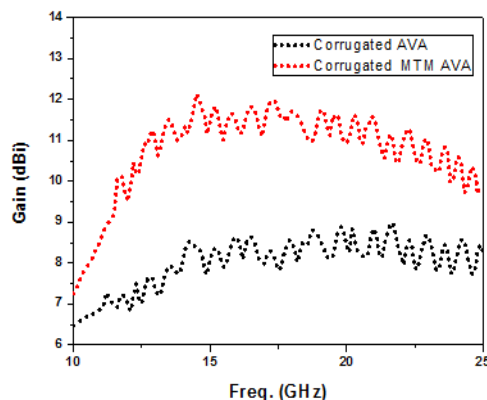
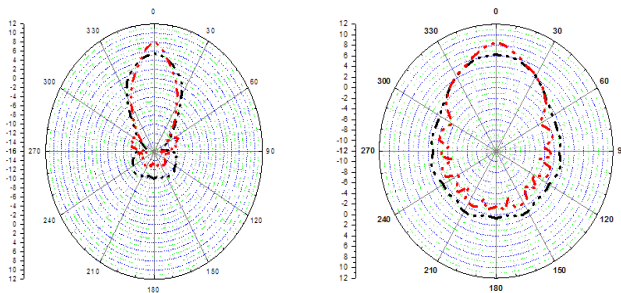
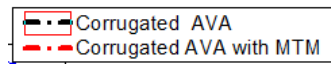


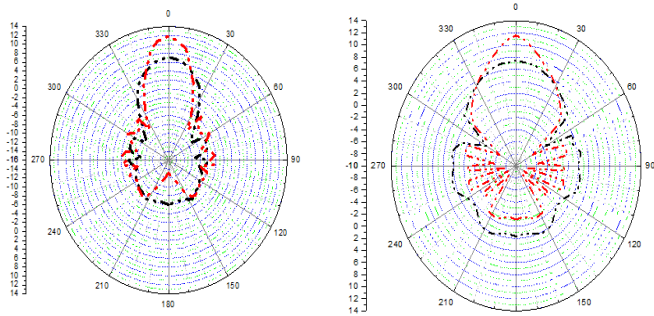
Figure 12. Comparison of Gain of Corrugated AVA and Corrugated MTM AVA

Figure 13 and Figure 14 illustrate the simulated radiation patterns of the corrugated AVA and the proposed MTM antenna on the E-plane and H-plane at 10, 15 and 25 GHz, respectively. It can be seen from the radiation pattern that loaded MTMs result in better directivity with improvement in gain [37] and possess enhanced radiation performance by suppressing the undesired side lobes [38] resulting in low side lobe levels.



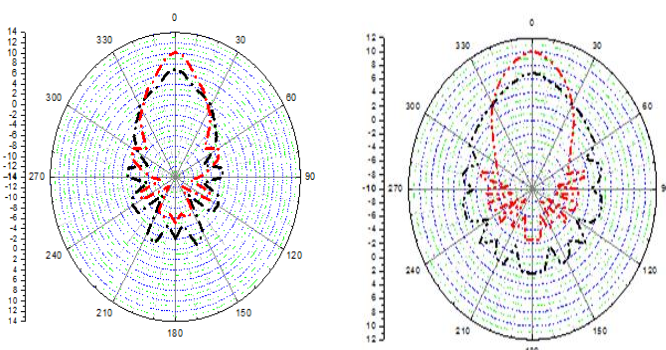
E Plane at 10 GHz

H Plane at 10 GHz



E plane at 15 GHz

H plane at 15 GHz



E Plane at 25 GHz

H Plane at 25 GHz

Figure 13. E plane radiation patterns

Figure 14. H plane radiation patterns

Thus, it is evident that the proposed antenna offers higher directivity, but it can be costlier due to the complex fabrication process.

VII. FABRICATION AND MEASURED RESULTS

To substantiate the simulated result as proposed in [1], the antenna is fabricated using substrate material FR4 with the relative dielectric constant of 4.4, $\tan \delta = 0.02$, and thickness of 1.6 mm. The antenna is fabricated by photolithographic technique [39]. The fabrication steps for the proposed antenna using photolithography process are briefly summarized: First, a computer aided design of the antenna geometry is made. A negative of this geometry printed on transparent sheet serves as the mask. Thereafter, a negative photo-resist film is laminated to the cleaned and dried copper clad substrate. The masked and photo-resist laminated copper clad substrate is exposed to ultra violet (UV) light. UV exposed photo-resist laminated copper clad substrate is developed. Finally, the developed copper clad substrate is chemically etched by Ferric Chloride $FeCl_3$ solution. Figure 15 (a, b) illustrates the photograph of the top and bottom layer of the fabricated antenna with overall dimensions as 22.60 mm x 15.80 mm.

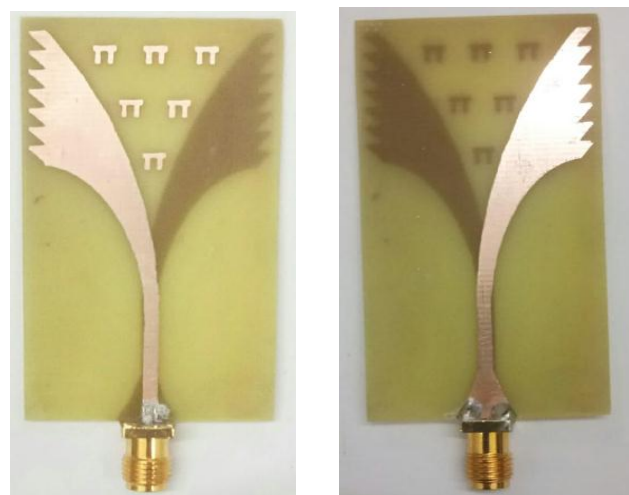


Figure 15. (a) Top (b) Bottom view of the fabricated antenna

Figure 16 depicts the simulated and measured S11 characteristics of the proposed antenna covering the entire band from 10 GHz - 25 GHz. Before carrying the measurement, the VNA (Agilent Fieldfox) was calibrated with a calibration kit with a short, open and loading apparatus, respectively. Subsequently, after the calibration process, the proposed antenna was connected to the VNA, and the S11 parameter results were obtained.

The measured return loss result displays that the proposed fabricated antenna achieves good impedance bandwidth ($S_{11} \leq -10$ dB) from 10 to 25 GHz though there is some decline in measured return loss. The maximum value of S_{11} lies in mid-range which is -21.4 dB at frequency of 18.2 GHz. The discrepancy between the simulation and measurement may be due to ohmic and substrate loss, surface roughness, and fabrication errors [40] mainly loading of metamaterials that may introduce distortion. Also, insertion loss of SMA connectors may contribute to the discrepancy in simulated and measured result [41]. Also, external disturbances and adjacently placed instruments may also contribute to the error.

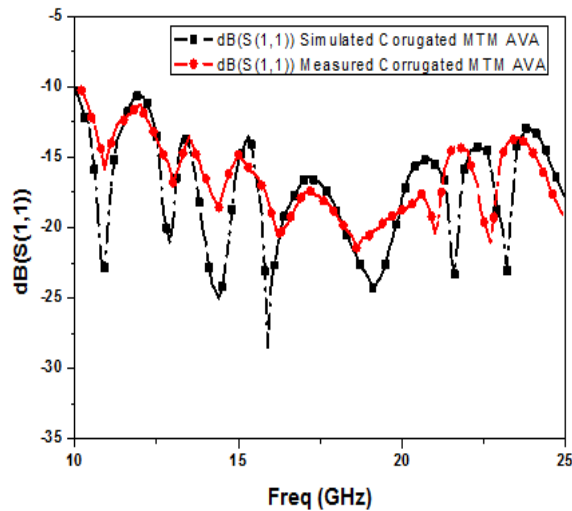


Figure 16. Comparison of Simulated and Measured return loss

Figure 17 depicts the comparison of the simulated and measured gain of the proposed corrugated AVA with novel metamaterial cells. The result shows good matching between the simulated and measured results except some minor loss in the measured result. The gain depends on the impedance matching, and since it is matched at mid frequencies, the match may be getting poorer at the lower and higher frequencies resulting in decline in gain at lower and upper frequency range. The measured gain of the antenna varies between 6.2 dBi – 10.7 dBi over 10 GHz – 25 GHz.

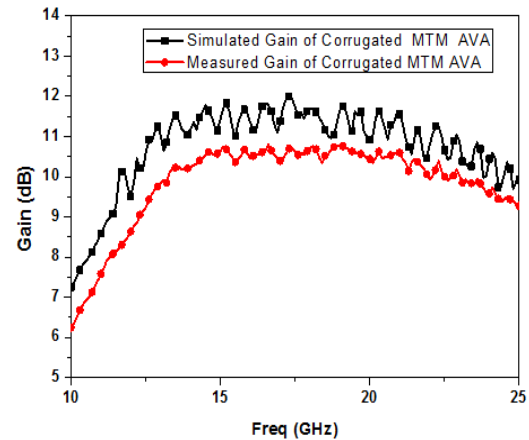


Figure 17. Comparison of simulated and measured Gain

The radiation characteristics of the proposed antenna are measured in the anechoic chamber and are shown in Figure 18. Radiation Patterns [42] are graphical representations of the distribution of radiated energy into space as a function of direction. The radiation pattern has two lobes: the main lobe where the maximum amount of radiated energy exists and the side lobes or minor lobes, where the radiation is distributed in a sideward and backward direction.

The AVA antenna which is antenna under test (AUT) and a RF transmitter system are placed at a known distance from the reference antenna. Horn antenna is used as the reference antenna, which is connected to a known receiver. The receiver system is employed to measure the power acquired by the antenna under test. A power meter to calculate the RF power is associated to the test antenna terminals by means of a co-axial cable and connectors. The positioning system is used to adjust the orientation of the AUT. The positioning system rotates the antenna under test and aids in the correct measurement of the AUT radiation pattern as a function of the angle.

Figures 18 and 19 display measured and simulated radiation patterns in the E and H planes at various AVA frequencies (10 GHz, 15 GHz, 25 GHz). As can be observed, the tapered slot's middle axis is where the maximum radiation occurs. Also, for E plane, the gain and HPBW increases with the frequency while for H plane it remains almost similar for various frequencies. As can be seen, the highest gain is in mid frequency range and drops for very low and high frequencies. The figure depicts improved radiation properties of the proposed antenna with high directivity and low sidelobe levels.

VIII. CONCLUSION

This paper proposes the analysis design and testing of a high gain corrugated AVA with novel epsilon negative (ENG) metamaterial. The ENG metamaterial enhances the reflection coefficient with a wider bandwidth from 10 to 25 GHz without increasing the size. Further, the proposed corrugated MTM AVA enhances the gain by approximately 3.8 dBi as compared to corrugated AVA in the desired frequency range. In this paper, first a conventional AVA (CAVA) is designed for desired frequency range. Thereafter, triangular corrugation is integrated and corrugated AVA is analyzed. Subsequently, its performance is further enhanced and analyzed by introducing Π shaped array of optimally placed metamaterial unit cells. Thereafter, the simulated design is fabricated using photolithography technique and the proposed fabricated antenna is tested for its return loss, gain and radiation pattern. The measured results are then compared with the HFSS simulated results. There is good agreement between simulated and measured results. The maximum gain achieved is approximately 10.7 dBi and antenna possesses high directional properties. As the proposed AVA design provides enhanced gain, improved return loss and compactness, it can be considered as a suitable candidate for satellite transmitter applications.

ACKNOWLEDGMENT

This work was undertaken during the tenure of an “ERCIM (The European Research Consortium for Informatics and Mathematics) Alain Bensoussan Fellowship” programme. Founded in 1988, ERCIM has members from leading European information technology and mathematics research establishments from 18 countries which provide research opportunities to brilliant PhDs from all over the world. Authors would also like to thanks to the microwave laboratory facilities at Fraunhofer Institute of Integrated Circuits (IIS), Germany. Fraunhofer society is the German research organization with 76 institutes spread throughout Germany and is Europe's largest application-oriented research organization.

REFERENCES

- [1] N. Muchhal, M. Elkhoully, Y. Fares and R. Z. Vintimilla, “Design of High Gain Corrugated Antipodal Vivaldi Antenna with Π Shaped Metamaterial for SATCOM Applications,” in Fifteenth International Conference on Advances in Satellite and Space Communications SPACOMM, April 24 - April 28, 2023, ISBN: 978-1-68558-035-3.
- [2] T. Rappaport, “Wireless communications - principles and practice,” 2nd Edition., Prentice Hall, 2002, ISBN 10: 0130422320.

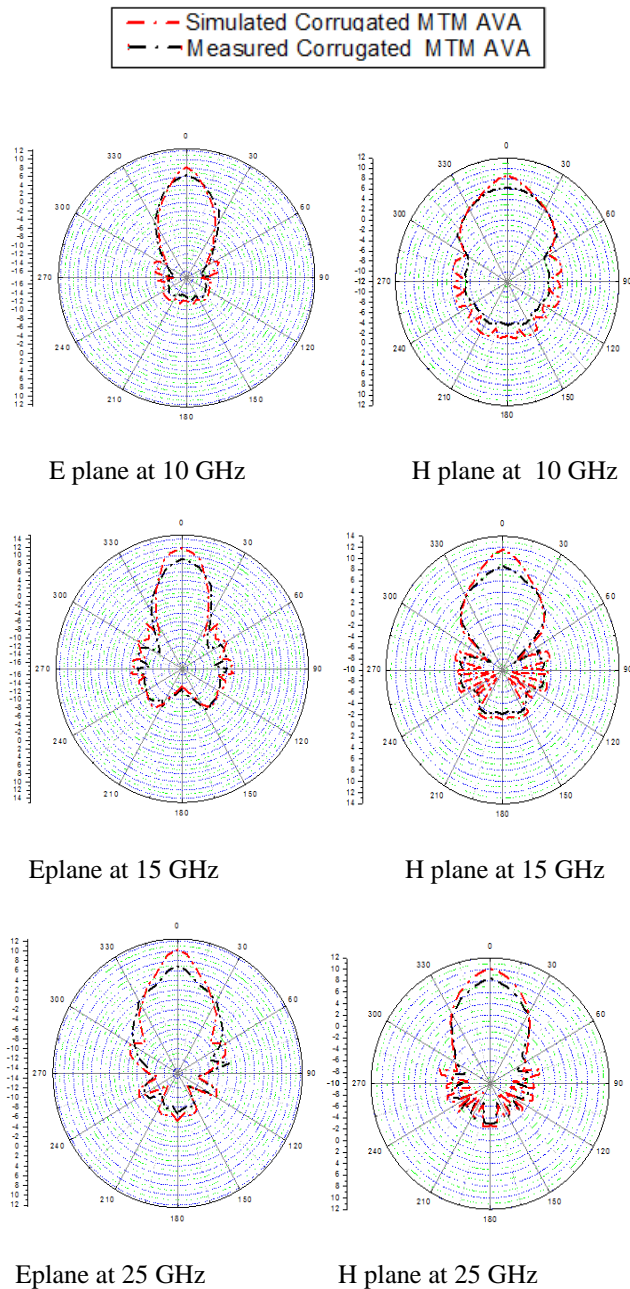


Figure 18. Simulated and measured E plane radiation pattern

Figure 19. Simulated and measured H plane radiation patterns

The results from simulation and measurement are in good agreement, except for slight discrepancy at higher frequencies caused by a fabrication error and the influence of the SMA connector on radiation characteristics. Hence, it is evident that the proposed fabricated antenna possesses higher directional properties with high gain.

- [3] A. F. Molisch, "Wireless Communications," 2nd Edition, John Wiley & Sons Ltd, Wiley-IEEE Press, New York, 2011, ISBN: 978-0-470-74187-0.
- [4] M. Donelli, S. Menon and A. Kumar, "Compact Antennas for Modern Communication Systems," Intl. Journal of Antenna and Propagation, Volume 2020 | Article ID 6903268.
- [5] D. Srikar and S. Anuradha, "A Compact Super Wideband Antenna for Wireless Communications," 2018 9th International Conference on Computing, Communication and Networking Technologies (ICCCNT), July 2018, pp. 1-4, DOI: 10.1109/ICCCNT.2018.8494146.
- [6] M. S. Elsayed et al., "Compact wide band antenna for millimetric communications," 2021 IOP Conf. Ser.: Mater. Sci. Eng. 1051 012032, DOI: 10.1088/1757-899X/1051/1/012032.
- [7] S. H. Son, U. H. Park, S. I. Jeon and C. J. Kim, "Mobile antenna system for Ku-band satellite Internet service," 2005 IEEE 61st Vehicular Technology Conference, Stockholm, Sweden, 2005, pp. 234-237, DOI: 10.1109/VETECS.2005.1543285.
- [8] R. D. Gaudenzi, C. E. and R. Viola, "Analysis of satellite broadcasting systems for digital television," in IEEE Journal on Selected Areas in Communications, vol. 11, no. 1, pp. 99-110, Jan. 1993, DOI: 10.1109/49.210548.
- [9] S. Vaccaro, F. Tiezzi, M. F. Rúa and C. D. G. De Oro, "Ku-Band Low-Profile Rx-only and Tx-Rx antennas for Mobile Satellite Communications," 2010 IEEE International Symposium on Phased Array Systems and Technology, October 2010, pp. 536-542, DOI: 10.1109/ARRAY.2010.5613316.
- [10] S. -Y. Qin and W. -J. Zhang, "Design Objectives of Antenna for Satellite Communication VSAT and USAT Earth Station," 2012 Second International Conference on Instrumentation, Measurement, Computer, Communication and Control, February 2012, pp. 635-637, DOI: 10.1109/IMCCC.2012.155.
- [11] K. -X. Li, Z. -J. Guo and Z. -C. Hao, "A Multipolarized Planar Phased Array for LEO SATCOM Applications," in IEEE Antennas and Wireless Propagation Letters, vol. 21, no. 11, pp. 2273-2277, Nov. 2022, DOI: 10.1109/LAWP.2022.3185208.
- [12] N. Muchhal, M. Elkhouly, K. Blau and S. Srivastava, "Design of Highly Selective Band-pass Filter with Wide Stop-band using Open Stubs and Spurlines for Satellite Communication (SATCOM) Applications," The Fourteenth International Conference on Advances in Satellite and Space Communications, SPACOMM, April 2022, ISBN: 978-1-61208-939-3.
- [13] H. Alsuraisry, W. -J. Lin, I. Huang and T. -W. Huang, "Design of Ka-band Transceiver for Satellite Communication," 2019 IEEE Jordan International Joint Conference on Electrical Engineering and Information Technology (JEEIT), April 2019, pp. 307-310, doi: 10.1109/JEEIT.2019.8717521
- [14] P. J. Gibson, "The Vivaldi Aerial," 9th European Microwave Conference, September 1979, pp. 101-105, DOI: 10.1109/EUMA.1979.332681
- [15] E. Gazit, "Improved design of the Vivaldi antenna," IEE Proceedings H-Microwaves, Antennas and Propagation, vol. 135(2), pp. 89-92, 1988, DOI: 10.1049/ip-h-2.1988.0020.
- [16] M. Agahi, H. Abiri, and F. Mohajeri, "Investigation of a new idea for antipodal Vivaldi antenna design," Int. J. Computer Elec. Eng., vol. 3, no. 2, 2011.
- [17] M. Moosazadeh, S. Kharkovsky, and J. T. Case, "Microwave and millimetre wave antipodal Vivaldi antenna with trapezoid-shaped dielectric lens for imaging of construction materials," IET Microwaves, Antennas & Propagation, 10(3), pp. 1-9, 2015, DOI: 10.1049/iet-map.2015.0374.
- [18] A. S. Dixit and S. Kumar, "A miniaturized antipodal Vivaldi antenna for 5G communication applications," 7th international conference on signal processing and integrated networks (SPIN), February 2020 pp. 800 - 803, DOI: 10.1109/SPIN.48934.2020.9071075.
- [19] X. Zhang, Y. Chen, M. Tian, Liu J, and H. Liu, "A compact wideband antipodal Vivaldi antenna design," International Journal of RF and Microwave Computer-Aided Engineering, vol. 29, issue 4, April 2019, <https://doi.org/10.1002/mmce.21598>.
- [20] A. S. Dixit, S. Kumar, S. Urooj, and S. A. Malibari, "A Highly Compact Antipodal Vivaldi Antenna Array for 5G Millimeter Wave Applications," Sensors, vol. 21, 2360, 2021, DOI: 10.3390/s21072360.
- [21] T. Nassar and T. M. Weller, "A Novel Method for Improving Antipodal Vivaldi Antenna Performance," in IEEE Transactions on Antennas and Propagation, vol. 63, no. 7, pp. 3321-3324, 2015, DOI: 10.1109/TAP.2015.2429749.
- [22] H. Emre and A. M. Emre, "High Gain Ultrawide Band Vivaldi Antenna Design for Mini/Micro Satellite Synthetic Aperture Radar Applications," IEEE 2019 9th International Conference on Recent Advances in Space Technologies (RAST), July 2019, pp. 491-495, DOI: 10.1109/RAST.2019.8767888.
- [23] H. Cheng, H. Yang, Y. Li and Y. Chen, "A Compact Vivaldi Antenna with Artificial Material Lens and Sidelobe Suppressor for GPR Applications," IEEE Access, vol. 8, pp. 64056-64063, 2020, DOI: 10.1109/ACCESS.2020.2984010.
- [24] H. Sakli, C. Abdelhamid, C. Essid and N. Sakli, "Metamaterial-Based Antenna Performance Enhancement for MIMO System Applications," in IEEE Access, vol. 9, pp. 38546-38556, 2021, DOI: 10.1109/ACCESS.2021.3063630.
- [25] H. Attia, O. Siddiqui, L. Yousefi and O. M. Ramahi, "Metamaterial for gain enhancement of printed antennas: Theory, measurements and optimization," 2011 Saudi International Electronics, Communications and Photonics Conference (SIEPC), April 2011, pp. 1-6, DOI: 10.1109/SIEPC.2011.5876888.
- [26] J. Shan, A. Xu and J. Lin, "A parametric study of microstrip-fed Vivaldi antenna," 2017 3rd IEEE International Conference on Computer and Communications (ICCC), December 2017, pp. 1099-1103, DOI: 10.1109/CompComm.2017.8322713.
- [27] D. H. Schaubert, "Endfire tapered slot antenna characteristics," 1989 Sixth International Conference on Antennas and Propagation, ICAP 89, April 1989, pp. 432-436 INSPEC Accession Number: 3416994.
- [28] S. Wang, X. D. Chen and C. G. Parini, "Analysis of Ultra Wideband Antipodal Vivaldi Antenna Design," Loughborough Antennas and Propagation Conference, April 2007, pp. 129-132, DOI: 10.1109/LAPC.2007.367448.
- [29] A. M. Abbosh, H. K. Kan, and M.E Bialkowski, "Design of compact directive ultra-wideband antipodal antenna," Microwave and Optical Technology Letters, vol. 48, issue 12, pp. 2448-2450, Dec. 2006, DOI: 10.1002/mop.21955.
- [30] A. S. Dixit and S. Kumar, "A Survey of Performance Enhancement Techniques of Antipodal Vivaldi Antenna," in IEEE Access, vol. 8, pp. 45774-45796, 2020, DOI: 10.1109/ACCESS.2020.2977167.
- [31] J. Bai, S. Shi, and D.W. Prather, "Modified compact antipodal Vivaldi antenna for 4-50 GHz UWB application," IEEE Trans. Microw. Theory Tech, vol. 59(4), pp. 1051-1057, 2011, DOI: 10.1109/TMTT.2011.2113970.

- [32] G. K. Pandey and M. K. Meshram, "A printed high gain UWB Vivaldi antenna design using tapered corrugation and grating elements," *International Journal of RF and Microwave Computer-Aided Engineering*, vol. 25 (7), pp. 610-618, September 2015, DOI: 10.1002/mmce.20899.
- [33] A. S. Dixit and S. Kumar, "The enhanced gain and cost-effective antipodal Vivaldi antenna for 5G communication applications," *Microwave and Optical Technology Letters*, vol. 62 (6), pp. 2365-2374, 2020, DOI: 10.1002/mop.32335.
- [34] N. Muchhal, and S. Srivastava, "Compact Substrate Integrated Waveguide Bandpass Filter with S-Shaped Broadside-Coupled Complementary Split Ring Resonators (BC-CSRR)," *International Journal of Microwave and Optical Technology (IJMOT)*, vol. 15, No. 5, pp. 440-448, Sept. 2020, DOI: IJMOT-2020-5-21976.
- [35] N. Muchhal, S. Srivastava, and M. Elkhoully, "Analysis and Design of Miniaturized Substrate Integrated Waveguide CSRR Bandpass Filters for Wireless Communication," in *Recent Microwave Technologies*. London, United Kingdom: IntechOpen, 2022, DOI: 10.5772/intechopen.104733.
- [36] M. Guo, R. Qian, Q. Zhang, L. Guo, Z. Yang, and Z. Wang, "High-gain antipodal Vivaldi antenna with metamaterial covers," *IET Microwaves, Antennas & Propagation*, vol. 13, issue 15, pp. 2654-2660, Sept. 2019, DOI: 10.1049/iet-map.2019.0449.
- [37] L. Chen, Z. Lei, R. Yang, J. Fan, X. Shi. "A broadband artificial material for gain enhancement of antipodal tapered slot antenna," *IEEE Trans. Antennas Propag.*, vol. 63(1), pp. 395-400, Oct. 2015, DOI: 10.1109/TAP.2014.2365044.
- [38] M. C. Johnson, S. L. Brunton, N. B. Kundtz and J. N. Kutz, "Sidelobe Canceling for Reconfigurable Holographic Metamaterial Antenna," in *IEEE Transactions on Antennas and Propagation*, vol. 63, no. 4, pp. 1881-1886, April 2015, DOI: 10.1109/TAP.2015.2399937.
- [39] G. K. Reddy, G. U. Bhargava and P. Sridhar, "Fabrication of patch antenna with circular polarization for wireless LAN applications," *International Conference on Electrical, Electronics, Communication, Computer, and Optimization Techniques (ICECCOT)*, December 2017, pp. 98-102, DOI: 10.1109/ICECCOT.2017.8284647.
- [40] K. Y. Yazdandoost and K. Sato, "Fabrication error in resonant frequency of microstrip antenna," *Proceedings of 2001 International Symposium on Micromechatronics and Human Science (Cat. No.01TH8583)*, September 2001, pp. 41-44, DOI: 10.1109/MHS.2001.965219.
- [41] S. K. Dhar, M. S. Sharawi and F. M. Ghannouchi, "Microwave Connector De-Embedding and Antenna Characterization [Education Corner]," in *IEEE Antennas and Propagation Magazine*, vol. 60, no. 3, pp. 110-117, June 2018, DOI: 10.1109/MAP.2018.2818002.
- [42] C. A. Balanis, "Antenna theory: Analysis and design," 4th ed. Wiley and Sons (USA), 2016, ISBN: 978-1-118-64206-1.